Contribution from the Department of Chemistry,
Tulane University, New Orleans, Louisiana 70118

Solution Photochemistry of Anionic Metal Carbonyl Hydride Derivatives. Substitution and Dimer Disruption Processes in μ-H[M(CO)$_5$]$_2^-$ (M = Cr and W)

DONALD J. DARENSBOURG* and MICHAEL J. INCORVIA

Received May 25, 1978

Dimer disruption and photosubstitution of a carbon monoxide ligand has been observed in μ-H[M$_2$(CO)$_{10}$]$^-$ derivatives (M = Cr and W) upon irradiation into the lowest energy electronic transition bands. The photosubstitution chemistry of these derivatives has been demonstrated to proceed with a high quantum efficiency for CO loss, Φ_{410} = 0.20 for M = Cr and Φ_{366} = 0.45 for M = W. On the other hand, the quantum efficiency for dimer disruption in the presence of CO to afford M(CO)$_6$ was considerably less, being 0.046 and 0.017 for the chromium and tungsten derivatives, respectively. When the incoming ligand was ^{13}CO, the principal species formed was μ-H[M$_2$(CO)$_9$(^{13}CO)]$^-$, where the ^{13}CO ligand is in an equatorial site. Both photoprocesses, dimer disruption and photosubstitution, were interpreted in terms of the net bonding changes arising from depopulation of the d$_\pi$ orbitals on the metals and the coincident population of the metal–metal antibonding component of the "closed" three-center bond of the M–H–M moieties.

Introduction

Interest in the binuclear transition-metal cluster compounds containing the hydride ligand has recently been evident from the several reports appearing in the literature probing the intimate properties of these species from both structural[1-5] and chemical reactivity[6-10] viewpoints. In particular, a reinvestigation by Dahl and his colleagues of the structure of the electron-deficient [Et$_4$N][HCr$_2$(CO)$_{10}$] complex by neutron diffraction has revealed that the bridging hydrogen atom is located about 0.3 Å from the center of the Cr–Cr bond (Figure 1).[2] A similar structure for [Et$_4$N][HW$_2$(CO)$_{10}$] has been confirmed by a neutron-diffraction analysis by Hart, Bau, and Koetzle.[11] On the other hand, the structure of the electron-precise [PPN][HFe$_2$(CO)$_8$] complex contains a bridging hydrogen atom in addition to two bridging CO groups.[12] Mechanistic studies of the reduction of α,β-unsaturated carbonyl compounds by this binuclear cluster, NaHFe$_2$(CO)$_8$, have been reported by Collman, Brauman, and co-workers.[10] Similarly, MHCr$_2$(CO)$_{10}$ (M = Na and K) has been shown to be an effective reagent for selectively reducing α,β-unsaturated aldehydes, ketones, esters, and nitriles.[9] Darensbourg and co-workers[7,8] have investigated CO ligand lability in the group 6B metal carbonylates, [Et$_4$N][HM$_2$(CO)$_{10}$], and found that substitution of CO follows a rate law that is first order in bridging hydride carbonylate and zero order with respect to the incoming group 5A ligand (L). The reactions which eventually afford M(CO)$_4$L$_2$ derivatives were demonstrated to proceed via [HM$_2$(CO$_9$L]$^-$ intermediates, e.g., the species [Et$_4$N][HMo$_2$(CO)$_9$PPh$_3$] was isolated and fully characterized.

Our interest in the chemical reactivity of these binuclear metal carbonly clusters stems from the presence of these species in solutions of M(CO)$_6$ (M = Cr, Mo, and W) and potassium hydroxide which serve as a homogeneous catalyst mixture for the energy-important water gas shift reaction.[13,14] Indeed, recent studies have shown that Cr(CO)$_6$ is more active than the Ru$_3$(CO)$_{10}$ catalyst.[15] Unfortunately the chromium carbonyl catalyst has a shorter lifetime, becoming inactive after 20–25 turnovers.[16] However, King and co-workers have shown W(CO)$_6$ to be quite effective under more rigorous conditions (170 °C, 8 atm).[17] A scheme for the complete catalytic cycle is shown below for a process carried out at atmospheric pressure. As noted in Scheme I, the intermediate species [Cr(CO)$_5$] can be trapped by CO to return to Cr(CO)$_6$ or by HCr(CO)$_5^-$ to afford μ-H[Cr(CO)$_5$]$_2^-$. Thus, in order to keep the cycle going it is necessary to effect the reaction of μ-H[Cr(CO)$_5$]$_2^-$ with CO to yield Cr(CO)$_6$. Therefore, we have investigated and wish to report in this communication the solution photochemistry of the μ-H[M(CO)$_5$]$_2^-$ derivatives with carbon monoxide where M = Cr and W.[16]

Scheme I

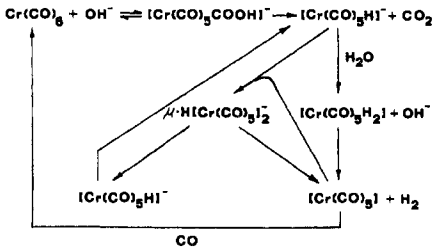

Experimental Section

Materials and Preparations. The tetraethylammonium salts of μ-H[M$_2$(CO)$_{10}$]$^-$ (M = Cr or W) were synthesized according to the method of Hayter.[6] The potassium salt of μ-H[Cr$_2$(CO)$_{10}$]$^-$ was prepared according to Grillone and Kedzia.[19] All salts were recrystallized twice prior to their use. Tetrahydrofuran was purified by distillation from sodium metal and benzophenone under nitrogen. Carbon monoxide (>90% ^{13}C) was obtained from Prochem, B.O.C. Ltd., London. Triphenylphosphine was recrystallized from hot methanol.

Instrumentation. Infrared spectra were recorded on a Perkin-Elmer 521 spectrophotometer equipped with a linear absorbance potentiometer. The spectra were calibrated against a water vapor spectrum below 2000 cm^{-1} and against a CO spectrum above 2000 cm^{-1}. Sodium chloride solution cells (0.1-mm path length) were used with THF solvent in the reference cell. Electronic absorption spectra were recorded on a Cary 14 spectrophotometer using 1-cm quartz cells.

Quantum Yield Determination. All irradiations were carried out on a merry-go-round apparatus equipped with Corning glass filters (either CS 5113 filters for 410 nm irradiations or CS 5840 filters for 366 nm irradiations) to isolate the desired spectral region of a Hanovia 450-W mercury lamp fitted with a uranium glass filter sleeve.

Each reported quantum yield is an average of three independent determinations. For each determination a stock solution approximately 3.5×10^{-3} M in μ-H[M$_2$(CO)$_{10}$]$^-$ was prepared. All solutions were made with freshly distilled THF (vide supra). Three-milliliter aliquots of the stock solution were pipetted into 13 × 100 mm test tubes fitted with serum caps and secured with copper wire. The tubes were then degassed of oxygen via three 30-min freeze–pump–thaw cycles. When carbon monoxide was the entering ligand the tubes were charged to a pressure slightly greater than atmospheric with CO at the end of the third freeze–pump–thaw cycle. In all other cases the tubes were charged with nitrogen gas. The test tubes were then loaded onto the merry-go-round where each tube was irradiated for a predetermined time period.

For each determination disappearance and/or appearance, curves were constructed (vide infra). In the dimer disruption studies only disappearance curves were constructed from the quantitative infrared

0020-1669/79/1318-0018$01.00/0

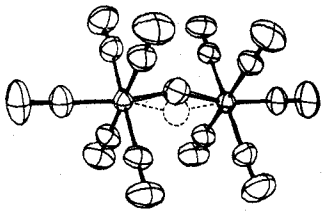

Figure 1. Geometry of μ-H[$Cr_2(CO)_{10}$]$^-$ determined as the tetraethylammonium salt (taken from ref 2).

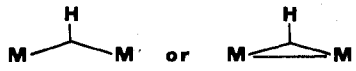

Figure 2. Pictorial description of the "closed" three-center, two-electron bond in the μ-H[$M_2(CO)_{10}$]$^-$ species.

monitoring of the concentration of μ-H[$M_2(CO)_{10}$]$^-$ (M = Cr or W) in solution from the intensity of either the E_u or A_{2u} mode at 1938 and 2043 cm^{-1} for μ-H[$W_2(CO)_{10}$]$^-$ and 1939 and 2031 cm^{-1} for μ-H[$Cr_2(CO)_{10}$]$^-$, respectively. The amount of hexacarbonyl produced during dimer disruption was quantitatively determined by monitoring the T_{1u} mode of $W(CO)_6$ at 1975 cm^{-1} or $Cr(CO)_6$ at 1980 cm^{-1}. In addition to constructing disappearance curves by the above procedure for photosubstitution, reaction appearance curves were also constructed for the photoproduction of equatorial μ-H[$M_2(CO)_9(^{13}CO)$]$^-$. The concentration of equatorial μ-H[$M_2(CO)_9(^{13}CO)$]$^-$ in solution was monitored by the intensity of its A′ mode at 2037 cm^{-1} and 2028 cm^{-1} for the tungsten and chromium analogues, respectively. All quantum yields were calculated from either an appearance or disappearance curve. Potassium ferrioxalate actinometry was used to measure the lamp flux.

Results and Discussion

Bonding and Electronic Structure. A single-crystal neutron diffraction study of [Et_4N][$HCr_2(CO)_{10}$] has recently been reported by Dahl and co-workers[2] which indicates the anion to be of D_{4h} symmetry (see Figure 1) with a bent symmetric Cr–H–Cr bond (Cr···Cr = 3.386 (6) Å). The structure of the tungsten analogue based on neutron diffraction data obtained at 14 K by Bau and colleagues[5,11] reveals that the bridging hydrogen atom is located 0.71 Å from the center of the W–W bond, with the W–H–W bond being quite asymmetric. The bonding in these and related derivatives has been described as a three-center, two-electron bond of a "closed" type involving the simultaneous symmetrical overlap of orbitals on the three atoms, directed toward the center of a triangle (Figure 2).[1,5,20,21] This description indicates partial M···M bonding character since there is just enough valence electrons in the moiety to fill the bonding molecular orbital and none to occupy either of the antibonding levels. The σ-bonding levels of the $M(CO)_5$ moieties have been chosen for bonding with the hydride ligand, that is the d_{z^2} orbitals (I). Nevertheless,

(I)

there could be some contribution from the orbitals involved in π bonding (d_{xz} or d_{yz}) with the M–CO framework (II).

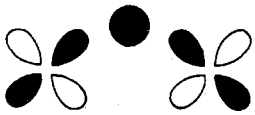

(II)

These orbitals are of the appropriate symmetry to interact with the hydride ligand orbital as has been previously noted.[3,22] Indeed this interaction may be anticipated to be of some importance because of the nonlinearity of the M–H–M bond (158.9° for Cr and 137.2° for W). Scheme II places the filled d_π orbitals of the two $M(CO)_5$ moieties higher in energy than the filled three-center bonding molecular orbital as proposed by Harris and Gray.[23]

Scheme II

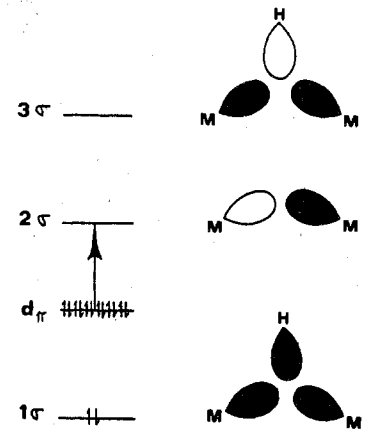

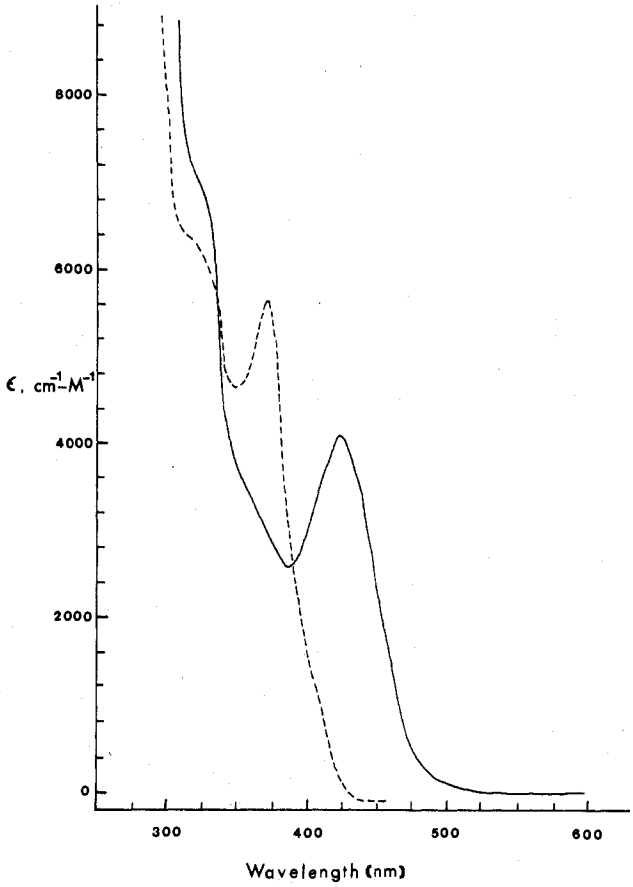

Figure 3. Electronic spectra at room temperature in THF of [Et_4N]$^+$$\mu$-H[$M(CO)_5]_2^-$ species: —, M = Cr; - - -, M = W.

The electronic absorption spectra of [Et_4N][$HW_2(CO)_{10}$] and [Et_4N][$HCr_2(CO)_{10}$] in THF are given in Figure 3. Harris and Gray[23] have assigned the 366-nm band in [Et_4N][$HW_2(CO)_{10}$] as a $d_\pi \rightarrow 2\sigma$ transition depicted in Scheme II. In a similar manner we are assigning the lowest energy absorption band in the chromium derivative at 423 nm (ϵ 4100) as a $d_\pi \rightarrow 2\sigma$ transition.

Solution Photochemical Studies. Both dimer disruption and photosubstitution of a carbon monoxide ligand were observed upon irradiation into the lowest energy electronic transition band of the μ-H[$M_2(CO)_{10}$]$^-$ complexes with the photochemical results being given in Table I. The photochemical

Table I. Dimer Disruption and Photosubstitution Quantum Yields for μ-H[$M_2(CO)_{10}$]$^-$ Derivatives[a]

salt	quantum yields: dimer disruption	quantum yields: photosubstitution
$[Et_4N][HCr_2(CO)_{10}]$[b]	0.036 ± 0.008	0.20 ± 0.10
$K[HCr_2(CO)_{10}]$[b]	0.046 ± 0.009	0.30 ± 0.10
$[Et_4N][HW_2(CO)_{10}]$[c]	0.017 ± 0.005	0.45 ± 0.09

[a] All reactions were carried out in THF. [b] Wavelength of irradiation, 410 nm. [c] Wavelength of irradiation, 366 nm. Errors in quantum yields represent one standard deviation.

dimer disruption reactions were studied in tetrahydrofuran saturated with carbon monoxide, where the quantum yields reported for this process are based on the disappearance of the bridging dimer. μ-H[$Cr_2(CO)_{10}$]$^-$ photodisproportionates in the presence of carbon monoxide to form $Cr(CO)_6$ and a green precipitate.[24] Stoichiometrically 1.1 ± 0.1 mol of $Cr(CO)_6$ are produced for every mole of $[Et_4N][HCr_2(CO)_{10}]$ which photodisproportionates. Similarly for the potassium salt the ratio is 1.3 ± 0.4 mol of $Cr(CO)_6$ for every mole of $K[HCr_2(CO)_{10}]$. Although the photodeclusterification quantum yield for the potassium salt is slightly larger than that for the tetraethylammonium salt, 0.046 ± 0.009 compared to 0.036 ± 0.008, it should be noted that these values are within one standard deviation of each other. The photochemical quantum efficiency for dimer disproportionation of $[Et_4N][HW_2(CO)_{10}]$ is 0.017 ± 0.005; that is, less than half that of the corresponding chromium analogues. The photoproduct of the dimer cleavage was $W(CO)_5THF$. However, it is not known if $W(CO)_5THF$ is immediately formed after dimer disproportionation or if the dimer fragments first scavenge carbon monoxide (reactions carried out in CO saturated THF) to form $W(CO)_6$ followed by photolysis at 366 nm to afford $W(CO)_5THF$. The presence of $W(CO)_5$-THF (ν(CO) of E mode at 1934 cm^{-1}) was detected by a broadening at the peak half height of the ν(CO) E_u mode of μ-H[$W_2(CO)_{10}$]$^-$ at 1941 cm^{-1} during photolysis. Therefore, in both cases the photochemical cleavage of the bridging dimer μ-H[$M_2(CO)_{10}$]$^-$ proceeds with a low quantum efficiency of a few hundredths. The fate of the hydride fragment in both the photochemical and thermal[7,8] dimer disruption processes has thusfar defied detection, i.e., no products of CO reduction have been observed. It is possible that traces of protic solvent(s) or hydroxyl groups on the surface of the glassware react with the M–H$^-$ component to afford H_2 (analogous to the process in Scheme I).

On the other hand, the photosubstitution of a carbon monoxide ligand proceeds with a large quantum efficiency of a few tenths. When μ-H[$W_2(CO)_{10}$]$^-$ was photolyzed at 366 nm in the presence of ^{13}CO, μ-H[$W(CO)_5$][$W(CO)_4(^{13}CO)$]$^-$ was formed (ν(CO) bands at 2038 (w), 1958 (m, sh), 1938 (vs), 1930 (s, sh), 1878 (m), and 1842 (w) cm^{-1}). The band pattern of the monosubstituted ^{13}C derivative (see Figure 4) matched that of the molybdenum analogue prepared in our laboratory from μ-H[$Mo_2(CO)_9PPh_3$]$^-$ and ^{13}CO.[25] The quantum yield for CO photosubstitution was calculated to be 0.45. In a similar manner, a carbon monoxide ligand may undergo photosubstitution with triphenylphosphine. When a 10:1 molar excess of PPh_3 to $[Et_4N][HW_2(CO)_{10}]$ was irradiated at 366 nm in THF, $[Et_4N][HW_2(CO)_9PPh_3]$ was formed (ν(CO) bands at 2060 (w), 2000 (w), 1928 (s, sh), 1923 (s), 1878 (m–s), and 1840 (m) cm^{-1}). Again, this band pattern of $[Et_4N][HW_2(CO)_9PPh_3]$ matched that of $[Et_4N][HMo_2(CO)_9PPh_3]$, a complex which has been fully characterized, having a PPh_3 ligand in an equatorial coordination site.[8] In an analogous manner the chromium bridging dimer underwent photosubstitution of a carbonyl ligand with

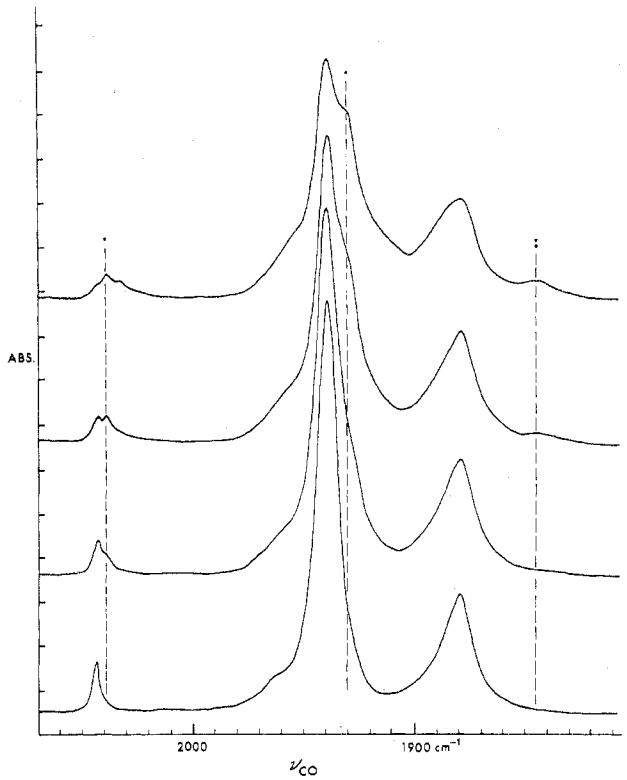

Figure 4. ν(CO) traces of the time-dependent photochemical incorporation of ^{13}CO into μ-H[$W(CO)_5]_2^-$ in THF solution. The bottom spectrum is that of the sample prior to irradiation (a similar trace was observed for the thermal blank). Peaks marked by a single asterisk correspond to equatorial ^{13}CO labeled species, whereas, the peak identified by a double asterisk corresponds to the axial ^{13}CO labeled species.

^{13}CO. The quantum yield for photosubstitution was 0.2 ± 0.1 in the tetraethylammonium salt and 0.3 ± 0.1 in the potassium salt at 410 nm. This observation may be indicative of enhanced ion pairing in the potassium salt; however, since the Φ values are within one standard deviation of each other no notable significance is attached to this quantum efficiency difference. However, when μ-H[$Cr_2(CO)_{10}$]$^-$ was photolyzed at 410 nm in THF with a 10 molar excess of triphenylphosphine, $Cr(CO)_5PPh_3$ and $Cr(CO)_4[PPh_3]_2$ were formed, probably as the result of severe steric interactions in the phosphine-substituted primary photoproduct, μ-H[$Cr_2(CO)_9PPh_3$]$^-$. Both photoprocesses, dimer disruption and photosubstitution, of the bridging dimers μ-H[$Cr_2(CO)_{10}$]$^-$ and μ-H[$W_2(CO)_{10}$]$^-$ can be interpreted in terms of the net bonding changes arising from depopulation of the highest occupied molecular orbital of the ground state and the coincident population of the lowest unoccupied molecular orbital of the respective complex. The qualitative ordering of the molecular orbital energy levels given in Scheme II will be used to illustrate such bonding changes.

The lowest energy electronic transition in the μ-H[$M_2(CO)_{10}$]$^-$ complexes (M = Cr and W) is represented by the promotion of an electron from the highest occupied molecular orbital d_π to the lowest unoccupied molecular orbital, designated 2σ in Scheme II ($\alpha d_{z^2} - \beta d'_{z^2}$ or $\alpha d_{xz} - \beta d'_{xz}$, or some admixture thereof). Since the d_π molecular orbitals represent the metals and their carbonyl ligands, depopulation of this bonding molecular orbital will weaken the metal–carbonyl π-bonding framework. Concomitantly, population of the 2σ level will add some antibonding character to the metal–metal bond of the μ-H[$M_2(CO)_{10}$]$^-$ dimer, thus weakening the metal–metal bond. It is important to note that this molecular orbital does not include any hydrogen 1s character and will therefore not affect the metal–hydrogen bonding network.

Scheme III

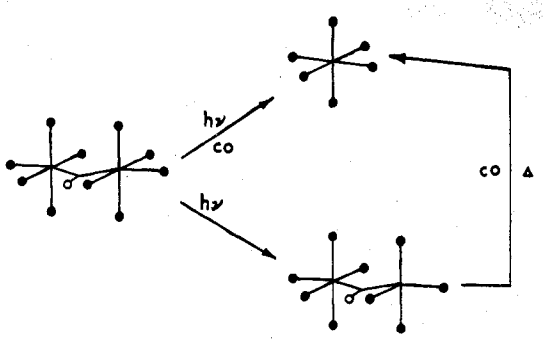

III

Therefore, the photosubstitution of carbon monoxide can be understood in terms of the above bonding changes; population of the 2σ orbital and depopulation of the d_π orbitals will weaken the σ and π bonding between metal and CO, respectively. This weakening of the M–CO bond is enough to facilitate the photosubstitution of a carbonyl ligand with a high quantum efficiency; 0.2 ± 0.1 for μ-$H[Cr_2(CO)_{10}]^-$ and 0.45 ± 0.09 for μ-$H[W_2(CO)_{10}]^-$.

On the other hand, the photodeclusterification reactions take place with a low quantum efficiency: 0.036 ± 0.008 for $[Et_4N][HCr_2(CO)_{10}]$ and 0.017 ± 0.005 for $[Et_4N][HW_2(CO)_{10}]$. The photodisproportionation of μ-$H[M_2(CO)_{10}]^-$ species is the direct result of population of the 2σ level, but this process leaves the metal–hydride component of the bridged structure intact and thus only affects the M–H–M bond to the extent that metal–metal interactions are important in this bonding sequence. It should be pointed out that we are unable to determine whether the disproportionation of the cluster is due to a primary photochemical process as discussed above or is due to a secondary thermal process after photolabilization of a carbonyl ligand (Scheme III). However, we have previously noted that species of the type III produced via loss of a labile PPh_3 group from μ-$H[Mo_2(CO)_9PPh_3]^-$ are effectively trapped with incoming ligands quantitatively.[25,26] Therefore, it is felt that photodeclusterification of the μ-$H[M_2(CO)_{10}]^-$ derivatives is most likely a primary photochemical process.

The lack of a quantitative production of $M(CO)_6$ from the heterolytic dimer disruption of μ-$H[M_2(CO)_{10}]^-$ in the presence of CO is assumed to be due to a more efficient secondary decomposition photochemical reaction of the $[HM(CO)_5]^-$ species, for these derivatives are known to be highly absorbing in the spectral region irradiated.[26] Thus, the photochemical route for returning to $M(CO)_6$ from μ-$H[M_2(CO)_{10}]^-$ in Scheme I, unlike that of the thermal pathway,[14] is not an efficient procedure for enhancing the catalytic cycle.

Some comments regarding the stereochemical site occupied by the incoming ^{13}CO ligand in the μ-$H[M_2(CO)_{10}]^-$ derivatives are in order. The assignment of the ν(CO) absorptions for the various ^{13}CO labeled species were based on the force field computation previously described for the μ-$H[Mo_2(CO)_{10}]^-$ derivative.[25] The infrared prediction for the site occupied by ^{13}CO in the molybdenum species, μ-$H[Mo_2(CO)_9(^{13}CO)]^-$, was further confirmed by ^{13}C NMR measurements. The ν(CO) force field fit is given in Table II for the μ-$H[W_2(^{12}CO)_{10-n}(^{13}CO)_n]^-$ (n = 0, 1, 2) species, while the respective spectral traces for the time-dependent incorporation of ^{13}CO into μ-$H[W_2(CO)_{10}]^-$ are shown in Figure 4. As is readily discernible by following the growth and decay of ν(CO) bands during the photolysis process, the primary product formed is μ-$H[W_2(CO)_9(^{13}CO)]^-$ where ^{13}CO is in an equatorial position. There was observed a small quantity of ^{13}C labeled material where the label was in an axial site (ν(CO) band indicated by a double asterisk in Figure 4). Similar observations were noted for both the chromium and tungsten bridging hydride species. The propensity of the incoming ^{13}CO ligand for an equatorial position either reflects a stereochemical preference for equatorial CO loss or a rapid rearrangement process occurring in the intermediate such that there is a vacant equatorial site.[27,28]

Table II. Calculated and Observed ν(CO) Vibrational Modes in μ-$H[W(CO)_5]_2^-$ Species[a]

molecule	vibration	ν(CO), cm^{-1} obsd[b]	ν(CO), cm^{-1} calcd
all ^{12}CO species (D_{4h})	A_{1g}		2044.9
	A_{2u}	*2041.4*	2040.3
	B_{1g}		1971.7
	B_{2u}	*1962.0*	1966.6
	E_u	*1937.7*	1938.4
	E_g		1933.2
	A_{1g}		1880.8
	A_{2u}	*1878.3*	1877.3
monosubstituted ^{13}CO,[c] equatorially (C_s)	A′		2043.2
	A′	*2037.6*	2034.2
	A′		1970.0
	A′		1961.9
	A″	*1937.7*	1938.4
	A′	*1930.0*	1935.9
	A″		1933.2
	A′		1907.2
	A′		1880.3
	A′	*1877.6*	1876.7
monosubstituted ^{13}CO, axially (C_{4v})	A_1		2044.2
	A_1		2039.3
	B_1		1971.7
	B_1		1966.6
	E		1938.4
	E		1933.2
	A_1		1879.1
	A_1	*1842.5*[d]	1838.6
disubstituted ^{13}CO, equatorially (C_1)[e]	A		2036.9
	A	*2031.7*	2032.5
	A		1965.1
	A		1960.5
	A		1935.9
	A		1935.9
	A		1907.4
	A		1906.9
	A		1879.5
	A		1876.2

[a] Spectra were determined in THF solvent. The refined CO force constants calculated were $k_1 = 14.37_1$, $k_2 = 15.66_1$, $k_c' = 0.26_9$, $k_c = 0.26_7$, $k_t = 0.53_2$, $K = 0.04_1$, and $k_j = -0.03_0$ with an average error in frequencies of 2.2 cm^{-1}. [b] Italicized frequencies were used as input in the refinement process. [c] Although all nine bands are predicted to be infrared active, the dipole moment changes are negligible for several of these symmetry modes. [d] A weak vibration observed in the enriched sample. [e] Other symmetries resulting from a difference in positioning of the two ^{13}CO ligands about the individual metal centers provide essentially identical predictions for the one uniquely observed ν(CO) band.

In summary a comparison of the thermal and photochemical ligand substitution and dimer disruption processes illustrates a great deal of similarity between the two modes for activating the μ-$H[M_2(CO)_{10}]^-$ derivatives.[7,8] The most efficient process in both cases is carbonyl ligand dissociation with the resultant intermediate having a vacant equatorial site for coordination, i.e., the equatorial CO site is preferentially enriched when the incoming ligand is ^{13}CO. Thermal ligand substitution reactions of the chromium and tungsten bridging hydrides with PPh_3 afford $M(CO)_4[PPh_3]_2$ complexes, thus indicating enhanced rates for dimer disruption as the parent μ-$H[M_2(CO)_{10}]^-$ species are substituted with triphenylphosphine. In contrast, for the larger tungsten metal center it is possible to photosubstitute CO with PPh_3 without disruption of the dimer (as was observed thermally for the molybdenum derivatives[8])

yielding μ-H[$W_2(CO)_9PPh_3$]$^-$, whereas μ-H[$Cr_2(CO)_{10}$]$^-$ in the presence of PPh_3 leads to the production of $Cr(CO)_4[PPh_3]_2$ upon either thermal or photochemical activation.

Acknowledgment. The authors are thankful for helpful discussions with Marcetta Y. Darensbourg, Robert R. Burch, Jr., and Joseph A. Froelich. The financial support of the National Science Foundation through Grant CHE 76-04494 and of Tulane University is greatly appreciated.

Registry No. [Et_4N][$HCr_2(CO)_{10}$], 16924-36-0; [Et_4N][$HW_2(CO)_{10}$], 12083-01-1; K[$HCr_2(CO)_{10}$], 61453-56-3; $W(CO)_5THF$, 36477-75-5; μ-H[$W(CO)_5$][$W(CO)_4(^{13}CO)$]$^-$, 68212-99-7; μ-H[$Cr(CO)_5$][$Cr(CO)_4(^{13}CO)$]$^-$, 68212-92-0; [Et_4N][$HW_2(CO)_9PPh_3$], 68212-91-9; $Cr(CO)_5PPh_3$, 14917-12-5; $Cr(CO)_4(PPh_3)_2$, 42029-71-0.

References and Notes

(1) J. P. Olsen, T. F. Koetzle, S. W. Kirtley, M. A. Andrews, D. L. Tipton, and R. Bau, *J. Am. Chem. Soc.*, **96**, 6621 (1974).
(2) J. Roziere, J. M. Williams, R. P. Stewart, Jr., J. L. Petersen, and L. F. Dahl, *J. Am. Chem. Soc.*, **99**, 4497 (1977).
(3) M. R. Churchill and S. W.-Y. Chang, *Inorg. Chem.*, **13**, 2413 (1974).
(4) H. B. Chin, Ph.D. Thesis, University of Southern California, Los Angeles, Calif., 1975.
(5) (a) R. Bau, R. G. Teller, S. W. Kirtley, and T. F. Koetzele, *Acc. Chem. Res.*, in press; (b) R. Bau and T. F. Koetzle, *Pure Appl. Chem.*, **50**, 55 (1978).
(6) R. G. Hayter, *J. Am. Chem. Soc.*, **88**, 4376 (1966).
(7) M. Y. Darensbourg and N. Walker, *J. Organomet. Chem.*, **117**, C68 (1976).
(8) M. Y. Darensbourg, N. Walker, and R. R. Burch, Jr., *Inorg. Chem.*, **17**, 52 (1978).
(9) G. P. Boldrini and A. Umani-Ronchi, *Synthesis*, 596 (1976).
(10) J. P. Collman, R. G. Finke, P. L. Matlock, R. Wahren, R. G. Komoto, and J. I. Brauman, *J. Am. Chem. Soc.*, **100**, 1119 (1978).
(11) D. W. Hart, R. Bau, and T. F. Koetzle, manuscript in preparation.
(12) H. B. Chin and R. Bau, *Inorg. Chem.*, **17**, 2314 (1978).
(13) D. J. Darensbourg and J. A. Froelich, *J. Am. Chem. Soc.*, **100**, 338 (1978).
(14) D. J. Darensbourg, M. Y. Darensbourg, R. R. Burch, Jr., J. A. Froelich, and M. J. Incorvia, *Adv. Chem. Ser.*, in press.
(15) R. M. Laine, R. G. Rinker, and P. C. Ford, *J. Am. Chem. Soc.*, **99**, 252 (1977).
(16) J. A. Froelich and D. J. Darensbourg, unpublished results. Initial activity of $Cr(CO)_6$ [0.39 mmol] in the presence of 9.6 mmol of KOH and 0.06 mol of H_2O in 15 mL of 2-ethoxyethanol at 100 °C was observed to be 32 mol of H_2/mol of $Cr(CO)_6$ per day.
(17) R. B. King, A. D. King, Jr., R. M. Hanes, and C. C. Frazier, 175th National Meeting, American Chemical Society, Anaheim, Calif., March 1978; C. C. Frazier, R. M. Hanes, R. B. King, and A. D. King, *Adv. Chem. Ser.*, in press.
(18) A preliminary report on the photochemistry of μ-H[$Cr(CO)_5]_2^-$ appeared in ref 14.
(19) M. D. Grillone and B. B. Kedzia, *J. Organomet. Chem.*, **140**, 161 (1977).
(20) R. A. Love, H. B. Chin, T. F. Koetzle, S. W. Kirtley, B. R. Whittesey, and R. Bau, *J. Am. Chem. Soc.*, **98**, 4491 (1976).
(21) L. B. Handy, J. K. Ruff, and L. F. Dahl, *J. Am. Chem. Soc.*, **92**, 7312 (1970).
(22) R. Mason and D. M. P. Mingos, *J. Organomet. Chem.*, **50**, 53 (1973).
(23) D. C. Harris and H. B. Gray, *J. Am. Chem. Soc.*, **97**, 3073 (1975).
(24) The formation of a green product (presumably containing chromium in its oxidized form) has been reported previously in the decomposition of anionic chromium carbonyl derivatives by Behrens and Weber (*Z. Anorg. Allg. Chem.*, **291**, 122 (1957)).
(25) D. J. Darensbourg, R. R. Burch, Jr., and M. Y. Darensbourg, *Inorg. Chem.*, **17**, 2677 (1978).
(26) M. Y. Darensbourg and R. R. Burch, Jr., unpublished results.
(27) D. J. Darensbourg and M. A. Murphy, *J. Am. Chem. Soc.*, **100**, 463 (1978).
(28) D. J. Darensbourg and M. A. Murphy, *Inorg. Chem.*, **17**, 884 (1978).

Contribution from the Department of Chemistry, University of Pittsburgh, Pittsburgh, Pennsylvania 15260

Intramolecular Associative Assistance in the Labilization of Chromium(III) Complexes: A Comparison of the Acid Aquation of 2,4-Pentanedione from Cr(hedta)(acac)$^-$ and Cr(edda)(acac)

JOE GUARDALABENE, SHIRLEY GULNAC, NANCY KEDER, and REX E. SHEPHERD*

Received August 4, 1978

The H_3O^+-assisted aquation of Hacac from Cr(hedta)(acac)$^-$ and Cr(edda)(acac) has been studied. An accelerated rate of about 10^3 relative to normal dissociative paths of Cr(III) complexes is observed for the Cr(hedta)(acac)$^-$ case. The pendant group effect for labilizing Cr(III), as proposed by Ogino and by Sykes, is proposed to account for the 10^3 enhancement. H_3O^+ scavenging of the distorted intermediates produced by pendant group association at Cr(III) is found to be much more rapid than the reverse reaction to the ground state. The Cr(hedta)(acac)$^-$ aquation occurs via two pendant arm-assisted pathways: (A) for Cr(hedtaH)(acac) and (B) for Cr(hedta)(acac)$^-$. The following kinetic parameters are obtained at μ = 0.20 ($NaClO_4$): $\Delta H_A^\ddagger$ = 21.34 ± 1.30 kcal/mol, $\Delta S_A^\ddagger$ = −0.89 ± 1.15 eu; $\Delta H_B^\ddagger$ = 16.68 ± 2.50 kcal/mol, $\Delta S_B^\ddagger$ = −21.39 ± 8.20 eu. The relative rates to achieve the distorted intermediates (k_2/k_1) is 51 in favor of assistance from the anionic carboxylate, the (B) path. The association constant for formation of Cr(hedta)(acac)$^-$ from Cr(hedta)(H_2O) and acac$^-$ was evaluated by competition with H_3O^+ to be (5.87 ± 0.24) × 10^5 M^{-1} (μ = 0.20, T = 25.0 °C). Bidentate acac$^-$ exhibits the normal chelate effect on the stability constant relative to monodentate anions, X$^-$, of ca. 2.9 × 10^4. The acid aquation of Cr(edda)(acac) proceeds by the normal dissociative pathway, scavenged by H_3O^+, in competition with return of the distorted intermediate to the ground state. At μ = 1.00 ($NaClO_4$), 25.0 °C, k_5 = 2.99 × 10^{-5} s^{-1} for the distortion step with k_{-5}/k_6, reversion to ground state vs. H_3O^+ scavenging, of 0.19. Comparisons are made to previous studies concerning the acid aquation of $Cr(acac)_3$.

Introduction

Cr(III) complexes having approximately octahedral environments are generally found to be of the substitution inert class. This is consistent with the large ligand field stabilization of the t_{2g}^3 configuration and the high activation enthalpy for a dissociative path which leads to ligand or solvent exchange. Ligand substitution at Cr(III) is moderately accelerated by oxyanions (SO_3^{2-},[1-3] NO_3^-,[4] NO_2^-,[5,6] carboxylates (RCO_2^-)[7,8]). The catalysis for the oxyanions for replacement of H_2O by entering nucleophiles, X$^-$, has been interpreted on the basis of anchimeric assistance provided by chelation of the oxyanion in the transition state.[2,3,7,8] Addition of X$^-$ to $CrY(H_2O)^{n-}$ (X$^-$ = $CH_3CO_2^-$, N_3^-, CrO_4H^-, MoO_4H^-, WO_4H^-; Y = hedta^{3-} or edta^{4-}) is observed to be much more rapid than the addition of X$^-$ to complexes such as $Cr(CH_3CO_2)(H_2O)_5^{2+}$ where the anchimeric effect is manifest.[9,10] Anation of $CrY(H_2O)^{n-}$ by X$^-$ is in the stopped-flow range. Addition of X$^-$ to $CrY(H_2O)^{n-}$ proceeds with apparent second-order rate constants ca. 10^3 larger than anation rates of $Cr(H_2O)_6^{3+}$ or $Cr(CH_3CO_2)(H_2O)_5^{2+}$.

The aminocarboxylate ligands have donor groups similar to the more common amino acid residues. Chromium may be assimilated by biological organisms from sources of environmental contamination (fly-ash, vegetable sources, mine

0020-1669/79/1318-0022$01.00/0